

Linear response functions for a vibrational configuration interaction state

Ove Christiansen^{a)} and Jacob Kongsted*Department of Chemistry, University of Århus, DK-8000 Århus C, Denmark*

Martin J. Paterson

School of Engineering and Physical Sciences, Heriot-Watt University, Edinburgh EH14 4AS, Scotland

Josep M. Luis

*Institute of Computational Chemistry, University of Girona, 17071 Girona, Spain
and Department of Chemistry, University of Girona, 17071 Girona, Spain*

(Received 19 September 2006; accepted 26 October 2006; published online 6 December 2006)

Linear response functions are implemented for a vibrational configuration interaction state allowing accurate analytical calculations of pure vibrational contributions to dynamical polarizabilities. Sample calculations are presented for the pure vibrational contributions to the polarizabilities of water and formaldehyde. We discuss the convergence of the results with respect to various details of the vibrational wave function description as well as the potential and property surfaces. We also analyze the frequency dependence of the linear response function and the effect of accounting phenomenologically for the finite lifetime of the excited vibrational states. Finally, we compare the analytical response approach to a sum-over-states approach. © 2006 American Institute of Physics. [DOI: 10.1063/1.2400226]

I. INTRODUCTION

The computation of accurate vibrational wave functions continues to attract much interest^{1–7} especially since it is now possible to obtain very accurate anharmonic potentials from high-level electronic structure computations. We are now in a position where we are able to compare directly the theoretical predictions of vibrational excitation energies and the vibrational contribution to molecular properties with experiment. Of particular relevance to these two issues we have recently developed a response theory for vibrational wave functions.⁸ The formal (second-quantized)⁶ equations of this vibrational response theory closely mirror those of electronic response theory.^{9–12} The response machinery can be applied to any explicit vibrational wave function, and we have previously shown this for vibrational self-consistent-field (VSCF) wave functions.⁸ In this paper we extend this into the correlated vibrational realm with the computation of linear response functions for vibrational configuration interaction (VCI) wave functions.

Response theory provides an attractive route to the computation of frequency-dependent molecular properties. Such molecular properties may have contributions from both electronic and vibrational degrees of freedom. These contributions can be separated by invoking the Born-Oppenheimer approximation and an additional approximation based on the large difference in typical size between electronic and vibrational energies (for a nonrotating and nontranslating molecule). Such separations have a long history and have seen widespread use.^{13–16} The result can be denoted as the clamped nuclei approximation and the response to the external fields is treated sequentially rather than simultaneously

with respect to electronic and vibrational contributions. In this way the polarizability can be separated into an electronic contribution averaged over vibrational motion and a pure vibrational contribution. In this regard vibrational response theory provides us with a means to compute the so-called pure vibrational (PV) contributions, which involve the electronic response functions as operators in the vibrational space. Technically this means that in addition to multidimensional electronic potential energy surfaces, we also require multidimensional electronic property surfaces. Thus, the computation of vibrational response functions becomes a formidable task.

Some applications usually ignore the pure vibrational contribution, for example Raman scattering at optical frequencies, based on the assumption that the PV contribution is negligible at optical frequencies. However, the PV contribution may be important for static properties, and may also be significant for an accurate description of frequency-dependent processes, e.g., the hyperpolarizabilities. Indeed, a number of research groups have recently focused on the evaluation of vibrational (hyper)polarizabilities.^{17–24}

Pure vibrational contributions to molecular properties have most often been calculated building on a harmonic oscillator description. Among the most popular approaches for going beyond the harmonic approximation is the use of a perturbation theoretical treatment of anharmonicity. For example, the approaches developed by Bishop and Kirtman for polarizabilities and hyperpolarizabilities are now in widespread use.^{15,16,25} An alternative procedure based on field induced nuclear relaxation geometry optimizations can be used to calculate static or infinite frequency vibrational (hyper)polarizabilities.^{26–29} Variational methods have been more limited in use, and primarily restricted to calculation of zero-point vibrational averages, see for example Ref. 30 and

^{a)}Electronic mail: ove@chem.au.dk

references therein. Finite field variational approaches have also been suggested and applied to the calculation of total static (hyper)polarizabilities.³¹

In this paper we implement analytical response theoretical methods for vibrational configuration interaction (VCI) methods. VCI has a long history and has been applied in many studies of vibrational energies, in particular, see Refs. 32–36 and references therein.

In Sec. II we describe the background theory before we in Sec. III describe the particular details of our implementation. Computational details are described in Sec. IV. We present sample calculations for water and formaldehyde in Sec. V, and finally we conclude with a summary and outlook in Sec. VI.

II. THEORY

A. General aspects

In this section we shall first summarize some general aspects of response theory to define our notation and relevant quantities. More detailed accounts of our response formalism are provided in Ref. 11 concerning general parametrizations in an electronic structure theory context and in Ref. 8 for vibrational response functions.

Consider an isolated molecular system described by a time-dependent Hamiltonian H

$$H = H_o + V^t. \quad (1)$$

H_o is the unperturbed Hamiltonian and V^t is a time-dependent perturbation operator of the form

$$V^t = \sum_y \epsilon_y(\omega_y) Y \exp(-i\omega_y t), \quad (2)$$

where ω_y is a frequency, Y is a perturbation operator (e.g., a component of the electric dipole operator), and ϵ_y is a strength parameter at our disposal. The time evolution of the system is governed by the time dependent Schrödinger equation

$$H|\bar{\Psi}_o(t)\rangle = i \frac{\partial}{\partial t} |\bar{\Psi}_o(t)\rangle. \quad (3)$$

The time-dependent expectation value $\langle \bar{\Psi}_o(t) | X | \bar{\Psi}_o(t) \rangle$ of a Hermitian operator X can be expanded in orders of the perturbation V^t ,

$$\begin{aligned} \langle \bar{\Psi}_o(t) | X | \bar{\Psi}_o(t) \rangle &= \langle \Psi_o | X | \Psi_o \rangle \\ &+ \sum_y \epsilon_y(\omega_y) \langle \langle X, Y \rangle \rangle_{\omega_y} \exp(-i\omega_y t) + \dots \end{aligned} \quad (4)$$

Here, $\langle \Psi_o | X | \Psi_o \rangle$ is the expectation value (e.g., a component

of the dipole moment) in the absence of V^t where the unperturbed wave function is denoted as $|\Psi_o\rangle$. The expansion coefficient $\langle \langle X, Y \rangle \rangle_{\omega_y}$ is the linear response function controlling the linear response of the expectation value $\langle \bar{\Psi}_o | X | \bar{\Psi}_o \rangle$ to the perturbation Y with associated frequency ω_y . In higher orders in the field strength nonlinear response functions enter the expansion in Eq. (4).

The linear and nonlinear response functions can be used for the calculation of a vast number of molecular properties. The ground-state frequency-dependent polarizability can be obtained from the negative of the linear response function by substituting components of the dipole moment operator (μ_i) for X and Y ($\alpha_{ij}(\omega) = -\langle \langle \mu_i, \mu_j \rangle \rangle_{\omega}$). For exact states, the linear response function for a reference state $|\Psi_o\rangle$ can be written in terms of the unperturbed eigenstates $\{|\Psi_o\rangle, |\Psi_k\rangle\}$ of H_o as

$$\langle \langle X, Y \rangle \rangle_{\omega_y} = P^{XY} \sum_k \frac{\langle \Psi_o | X | \Psi_k \rangle \langle \Psi_k | Y | \Psi_o \rangle}{\omega_y - \omega_k}. \quad (5)$$

The operator P^{XY} generates the two permutations of the operators and related frequencies (X, ω_x), (Y, ω_y) where $\omega_x = -\omega_y$. In Eq. (5) $\omega_k = E_k - E_o$, where E_o is the reference state energy and E_k is the eigenenergy of state Ψ_k . The linear response function has poles at $\omega_y = \pm \omega_f$, where ω_f is the energy for the transition from the reference state to the f th state [one specific state in the sum of Eq. (5)]. The residues of the linear response functions can be used to obtain probabilities for transitions between the reference state and the other eigenstates. Transition properties between two states different from the reference state require the consideration of the second residue of the quadratic response function, while two-photon absorption can be described through the first residue of this response function.

B. Separation of electronic and vibrational motions in response functions

We now consider the case where the state space considered is the space for both electronic and vibrational nuclear motions. Following the Born-Oppenheimer approximation the wave function is written as a product of an electronic wave function denoted by large letter bra-kets $|K\rangle$ and an accompanying vibrational wave function denoted $|k_K\rangle$. The electronic wave function and energies depend on the nuclear coordinates creating a dependency of electronic energies and properties on the coordinates for the internal motion. We shall in this paper not consider rotational motion explicitly.

Denoting the energy difference between the (K, k_K) state and the (O, o_O) state by ω_{k_K} and the pure electronic energy difference as ω_K we obtain

$$\begin{aligned} \langle\langle X, Y \rangle\rangle_{\omega_y} = P^{XY} & \left\{ \sum_{K, k_K \neq O, o_O} \frac{\langle o_O | \langle O | X | K \rangle | k_K \rangle \langle k_K | \langle K | Y | O \rangle | o_O \rangle}{\omega_y - \omega_{k_K}} \right\} \approx P^{XY} \left\{ \sum_{k_O \neq o_O} \frac{\langle o_O | \langle O | X | O \rangle | k_O \rangle \langle k_O | \langle O | Y | O \rangle | o_O \rangle}{\omega_y - \omega_{k_O}} \right. \\ & \left. + \left\langle o_O \left| \sum_{K \neq O} \frac{\langle O | X | K \rangle \langle K | Y | O \rangle}{\omega_y - \omega_K} \right| o_O \right\rangle \right\} = \langle\langle O | X | O \rangle, \langle O | Y | O \rangle \rangle_{\omega_y}^v + \langle o_O | \langle\langle X, Y \rangle\rangle_{\omega_y}^e | o_O \rangle = \langle\langle X, Y \rangle\rangle_{\omega_y}^v + \langle\langle X, Y \rangle\rangle_{\omega_y}^{e+va}. \quad (6) \end{aligned}$$

This is a standard derivation found in many works and textbooks.^{13–15,37} In Eq. (6) it is assumed that the vibrational energy differences are small compared to the electronic energy differences. This allows the use of closure over the vibrational states in the excited electronic state K . With the above assumptions the linear response function becomes a sum of two terms. The first term is a “pure vibrational” contribution, depending only on the vibrational states of the ground electronic state. The operators in the vibrational space are the electronic expectation values $\langle O | X | O \rangle$ and $\langle O | Y | O \rangle$ that are functions of the nuclear coordinates. The second term is the vibrational average value of the electronic property over the vibrational wave function of the ground electronic state.

In a recent paper we have described how to calculate vibrational average properties using VCI wave functions, including the construction of the relevant operators.³⁰ In the following we now describe how to calculate the pure vibrational part.

C. Response functions for vibrational configuration interaction wave functions

To describe anharmonic vibrational wave functions we use in this paper vibrational configuration interaction (VCI) based on a VSCF reference state. Thus we consider a system with M degrees of freedom, denoted modes (i.e., $3N-6$ or $3N-5$ for linear molecules, where N is the number of atoms of the molecules). For each mode we have a set of one-mode functions denoted modals.³⁴ The VSCF reference state is based on a direct product ansatz for the wave function in terms of one modal for each mode. Applying the variational principle to the VSCF ansatz provides working equations for obtaining the optimal one-mode functions. The VSCF accounts for anharmonicities between different modes in an average sense similar in spirit to the mean-field description of electronic interactions in self-consistent-field electronic wave function theory.

To provide a more accurate treatment of anharmonicity including vibrational dynamical correlation we employ a VCI approach. The correlations between the different modes beyond an average field description ignored in VSCF are included by taking into account in VCI excitation from occupied VSCF modals into “virtual” modals—unoccupied levels in the VSCF.

The full space of the VSCF state and its orthogonal complement of M -mode states may be written as $\{|\Phi\rangle, |\Phi_k\rangle\}$ where $|\Phi_k\rangle$ denotes M -mode states obtained from the VSCF

reference state by exciting from occupied to unoccupied modals. The VCI wave function can be written as a linear expansion in this space

$$|\Psi\rangle = C|\Phi\rangle + \sum_k C_k|\Phi_k\rangle. \quad (7)$$

Standard normalization to unit norm requires $1 = |C|^2 + \sum_k |C_k|^2$. Including the full sum over all excitations the full VCI (FVCI) wave function is recovered. Computationally cheaper VCI treatments include only a part of the full excitation space, for example, restricting the VCI expansion to excitations less or equal than a certain maximum excitation level n , and such VCI wave functions are denoted VCI[3]. The C parameters can be determined from the Schrödinger equation by projection or by variational criteria giving standard configuration interaction eigenvalue equations.

For the sake of deriving response functions in a manner coherent with the previous work on derivation of response functions for vibrational wave functions we write the VCI wave function in an exponential time-dependent parametrization as

$$|\bar{\Psi}(t)\rangle = \exp(-iP(t))\exp(\Lambda(t))|\Psi\rangle, \quad (8)$$

where $|\Psi\rangle$ is a VCI reference state, and the general phase $P(t)$ is a real function of time. The Λ operator carries out the transformation and is given as

$$\Lambda(t) = \sum_j (\lambda_j(t)Q_j^\dagger - \lambda_j^*(t)Q_j) \quad (9)$$

in terms of time-dependent parameters $\lambda(t)$ and the VCI state-transfer operators

$$Q_j^\dagger = |\Psi_j\rangle\langle\Psi|, \quad (10)$$

$$Q_j = |\Psi\rangle\langle\Psi_j|. \quad (11)$$

Here the set of states $|\Psi_j\rangle$ is an orthogonal complement to the reference VCI state $|\Psi\rangle$. Note that in this parametrization the VSCF modals of the VCI reference state modals are not allowed to relax to the perturbation. The pros and cons of such unrelaxed response approaches are discussed in Ref. 11.

With this form for the wave function the derivation of vibrational response functions falls under the general derivations in Ref. 8. We report here the general expressions obtained and equations specialized for VCI using the VCI state-transfer operators above.

The linear response function is

$$\langle\langle X, Y \rangle\rangle_{\omega_y} = \boldsymbol{\eta}^X \boldsymbol{\lambda}^Y(\omega_y) = \sum_{\pm i} \eta_i^X \lambda_i^Y(\omega_y) \quad (12)$$

with the accompanying first order response equation

$$\{\mathbf{E}^{[2]} - \omega_y \mathbf{S}^{[2]}\} \boldsymbol{\lambda}^Y(\omega_y) = \mathbf{g}^Y. \quad (13)$$

The $\mathbf{E}^{[2]}$ and $\mathbf{S}^{[2]}$ matrices can be written as

$$\mathbf{E}^{[2]} = \begin{bmatrix} \mathbf{A} & \mathbf{B} \\ \mathbf{B}^* & \mathbf{A}^* \end{bmatrix} = \begin{bmatrix} \mathbf{A} & \mathbf{0} \\ \mathbf{0} & \mathbf{A} \end{bmatrix}, \quad (14)$$

$$\mathbf{S}^{[2]} = \begin{bmatrix} \boldsymbol{\Sigma} & \boldsymbol{\Delta} \\ -\boldsymbol{\Delta}^* & -\boldsymbol{\Sigma}^* \end{bmatrix} = \begin{bmatrix} \mathbf{1} & \mathbf{0} \\ \mathbf{0} & -\mathbf{1} \end{bmatrix}, \quad (15)$$

where $A_{ij} = E_{-ij}^{[2]}$, $B_{ij} = E_{-i-j}^{[2]}$, $\Sigma_{ij} = S_{-ij}^{[2]}$ and $\Delta_{ij} = S_{-i-j}^{[2]}$ with the special ordering that has become standard.^{10,11,38} The right index j is ordered with excitation before deexcitation, ($j > 0$ before $j < 0$) and the left index i is ordered with deexcitation before excitation ($i < 0$ before $i > 0$). The first part of the above equations are the general equations for an exponentially parametrized state, and the last equality holds for a VCI state (assumed to be real). For VCI the excitation and deexcitation spaces decouple, since the $\boldsymbol{\Delta}$ and \mathbf{B} matrices become identically zero. In addition, the equations are simplified by the $\boldsymbol{\Sigma}$ matrix becoming unity. The only nontrivial matrix elements required in VCI linear response are therefore

$$A_{ij} = \langle \Psi | [Q_i, [H_o, Q_j^\dagger]] | \Psi \rangle = \langle \Psi_i | H_o | \Psi_j \rangle - \delta_{ij} \langle \Psi | H_o | \Psi \rangle, \quad (16)$$

$$\boldsymbol{\eta}^Y = \begin{pmatrix} \eta_i^Y \\ \eta_{-i}^Y \end{pmatrix} = \begin{pmatrix} \langle \Psi | [Y, Q_i^\dagger] | \Psi \rangle \\ \langle \Psi | [Y, Q_i] | \Psi \rangle \end{pmatrix} = \begin{pmatrix} \langle \Psi | Y | \Psi_i \rangle \\ -\langle \Psi_i | Y | \Psi \rangle \end{pmatrix}, \quad (17)$$

$$\mathbf{g}^Y = \begin{pmatrix} \eta_{-i}^Y \\ \eta_i^Y \end{pmatrix} = \begin{pmatrix} \langle \Psi | [Y, Q_i] | \Psi \rangle \\ \langle \Psi | [Y, Q_i^\dagger] | \Psi \rangle \end{pmatrix} = \begin{pmatrix} -\langle \Psi_i | Y | \Psi \rangle \\ \langle \Psi | Y | \Psi_i \rangle \end{pmatrix}. \quad (18)$$

The position of the poles of the VCI linear response function determines the VCI response excitation energies, which in turn are obtained from the generalized eigenvalue equation

$$\mathbf{E}^{[2]} \mathbf{U} = \mathbf{S}^{[2]} \mathbf{U} \Omega. \quad (19)$$

Here Ω is a diagonal matrix with the excitation energies on the diagonal, $\Omega_{ii} = \omega_i$, $\Omega_{-i-i} = -\omega_i$. For a particular final state f the transition moments are found from the residues of the response functions as

$$T_{fo}^Y = \sum_{\pm i} U_i^f \eta_i^Y. \quad (20)$$

Since the excitation and deexcitation spaces decouple for VCI the linear response equations can be limited to solving only in the excitation space. Thus, the linear equations to be solved can be limited to the following equations in half dimension:

$$\sum_{j>0} \{A_{ij} - \omega_y \delta_{ij}\} \lambda_j^Y(\omega_y) = \eta_{-i}^Y, \quad (21)$$

for $\pm \omega_y$. Here also $i > 0$. The response eigenvalue equations become similarly a matter of finding the eigenvalues of the \mathbf{A} matrix

$$\mathbf{A} \mathbf{U} = \mathbf{U} \Omega, \quad (22)$$

where \mathbf{U} and Ω are now only in the half dimension of the previous response equations. Note that this dimensionality corresponds to the number of free parameters of a normal VCI wave function optimization for a real state.

For VCI we see from Eq. (16) that diagonalizing the VCI \mathbf{A} matrix is equivalent to the standard approach of finding excited states by diagonalizing the VCI Hamiltonian matrix. In this context we shall, however, implement the VCI response variant as described in the next section.

III. IMPLEMENTATION

Our implementation is based on the direct VCI implementation described in Ref. 7. The concept of direct CI, which is in widespread use in electronic structure theory,^{39,40} refers to the fact that the full Hamiltonian matrix is never calculated and stored explicitly. Instead the VCI eigenvalue equations are solved iteratively performing linear transformations with trial vectors using a Davidson update⁴¹ for generating new trial vectors. The linear equation systems can be solved using similar direct techniques. This means that we use such iterative methods for solving Eqs. (21) and (22). For calculating the required vectors and matrix transformations we have at our disposal routines for calculating vectors of the following type:

$$\sigma_k = \sum_l \langle \Phi_k | H_o | \Phi_l \rangle C_l. \quad (23)$$

This scheme is general such that other operators than the Hamiltonian can be introduced in the transformation if they are of the same form.

We have implemented Hamiltonians and other operators of the “sum-over-products” form

$$H_o = \sum_{t=1}^{N_t} c_t \prod_{m=1}^M h_t^m, \quad (24)$$

where N_t denotes the number of terms and h_t^m denotes the one-mode operator working in space of mode m relevant for the term t . Polynomial expansions of the potential operator in normal coordinates are a special case of these formulas. Equivalent formulas can also be used to express the electronic expectation values of operators (e.g., electric dipole operators) in normal modes. The calculation of the operators is not the topic of this paper, but it should be clear that efficient interfacing of the presented theory to modern electronic structure programs is possible. For example, we have recently reported an automated calculation of potential and other operators in this form through the numerical calculation of geometrical derivatives of the electronic energies and electronic properties.³⁰ Both potentials and property operators are read from files and can therefore be provided by other means. Further details of the operator handling are described in other papers.^{7,42}

It should be noted that the above discussed direct methods refer to constructing the transformation in the basis of the VSCF reference ket and states defined by excitation out of this state. We denote this as the primitive basis. However,

the VCI response theory expressions of the previous section refer to the VCI reference state and the orthogonal complement to the VCI state. We choose to call this the orthogonal complement basis. We now describe how we can obtain vectors and transformations in the orthogonal complement from similar vectors and transformations in the primitive basis.

Assuming the VCI reference state is written as in Eq. (7) (with real positive coefficients for the VSCF reference state—a more general phase can be handled by the phase factor prefactor) the orthogonal complement space can be constructed using^{9,40}

$$|\Psi_k\rangle = |\Phi_k\rangle - \frac{C_k^*}{1+C}(|\Phi\rangle + |\Psi\rangle), \quad (25)$$

as can easily be checked. The orthogonal complement states are normalized and orthogonal to both the reference VCI state, $|\Psi\rangle$, and to each other. The states $|\Phi_k\rangle$ are the states obtained by the primitive modal excitations out of the VSCF state.

Vectors in the orthogonal complement basis can be transformed to the primitive basis, and the relevant matrix elements and transformations carried out before transforming the resulting vector from the primitive basis back to the orthogonal complement basis. Thus, an arbitrary state can be written in either basis

$$|b\rangle = b_o^{\text{oc}}|\Psi\rangle + \sum_k b_k^{\text{oc}}|\Psi_k\rangle = b_o^{\text{prim}}|\Phi\rangle + \sum_k b_k^{\text{prim}}|\Phi_k\rangle \quad (26)$$

and the coefficients of the two bases are related through

$$\mathbf{b}^{\text{prim}} = \begin{pmatrix} b_o^{\text{prim}} \\ b_k^{\text{prim}} \end{pmatrix} = \begin{pmatrix} b_o^{\text{oc}}C - \sum_{k>0} C_k^* b_k^{\text{oc}} \\ b_o^{\text{oc}}C_k + b_k^{\text{oc}} - \left[\sum_{l>0} C_l^* b_l^{\text{oc}} / (1+C) \right] C_k \end{pmatrix}, \quad (27)$$

$$\mathbf{b}^{\text{oc}} = \begin{pmatrix} b_o^{\text{oc}} \\ b_k^{\text{oc}} \end{pmatrix} = \begin{pmatrix} C b_o^{\text{prim}} + \sum_{k>0} C_k^* b_k^{\text{prim}} \\ b_k^{\text{prim}} - C_k b_o^{\text{prim}} - \left[\sum_{l>0} C_l^* b_l^{\text{prim}} / (1+C) \right] C_k \end{pmatrix}. \quad (28)$$

In this way vectors can be transformed back and forth from the primitive basis to the orthogonal complement basis (in our case $b_o^{\text{oc}}=0$) with comparatively low cost involving essentially only a few vector dot products and scalar times vector operations.

The above formalism is implemented in the MIDASCP program.⁴³ Also a sum-over-states (SOS) approach is implemented where the VCI linear response (LR) excitation energies and transition properties are calculated and the results are summed up to provide a SOS result for the response function [direct evaluation of Eq. (5)]. The LR and SOS results must be identical when all the states are included in the SOS formulas. While such an approach will be less efficient it may still be interesting to compare the result of SOS

and analytical response approaches at different levels, and may be a useful way to introduce finite vibrational lifetimes via phenomenological damping factors.

IV. COMPUTATIONAL DETAILS

The method described in the previous sections has been applied to the calculation of pure vibrational contributions to the polarizabilities of water and formaldehyde. The isotropic frequency-dependent linear polarizability is defined by $\bar{\alpha} = \frac{1}{3}(\alpha_{xx} + \alpha_{yy} + \alpha_{zz})$. The potential and property surfaces from CCSD/aug-cc-pVTZ or CCSD(T)/aug-cc-pVTZ calculations reported in Ref. 30 are used. Reference 30 also discusses the calculation of zero-point vibrational contributions to these properties.

The vibrational structure calculations have been performed using either VSCF or VCI linear response function methods. Harmonic oscillator (HO) one-mode basis sets were used where the harmonic oscillator exponents in each case were chosen in accordance with the harmonic part of the given potential. The size of the basis is characterized by the HO quantum number. From the primitive HO basis the VSCF calculation provides a set of modals to be used in the VCI calculations.

In addition to the calculations of the PV polarizability we also consider the total polarizability, i.e., the sum of the pure electronic polarizability, the zero-point vibrational average (ZPVA) correction, and the PV polarizability. The ZPVA polarizabilities have been taken from Ref. 30 and are based on CCSD/d-aug-cc-pVTZ (water) and CCSD/aug-cc-pVTZ (formaldehyde) electronic response functions.

The equilibrium structures of either water or formaldehyde were placed in the yz plane. The z axis was chosen as the C_2 axis and the molecules were placed with the center of mass in the origin, with the hydrogens confined to positive z values.

V. SAMPLE CALCULATIONS

In the following we present an analysis of the linear response based pure vibrational polarizability of water and formaldehyde in terms of the size of the one-mode basis set, mode-mode correlation level, truncation of the potential and property surfaces, and frequency dependence. Following this analysis we consider the sum-over-states formulation of pure vibrational polarizabilities and compare our results with other methods of calculations.

A. Analyses of the linear response pure vibrational polarizabilities

1. One-mode basis analysis

In Table I we report the pure vibrational contribution to the static polarizability for water and formaldehyde for a number of different one-mode basis sets of different sizes at the VCI[3] level (FVCI for water). The potential and property surfaces have been obtained using CCSD/aug-cc-pVTZ. We have in all VCI calculations included all VSCF modals. For both water and formaldehyde we observe a fairly fast convergence with respect to the size of the basis set, e.g., using only six HO basis functions leads to converged results

TABLE I. The static PV polarizability for water (V3M4T/P3M4T) and formaldehyde (V4M4T/P4M4T) calculated using VCI[3] and different numbers of one-mode basis functions per mode, N_m . The potential and property surfaces have been obtained using CCSD/aug-cc-pVTZ. The results are in a.u.

N_m	Water			Formaldehyde			
	α_{yy}	α_{zz}	$\bar{\alpha}$	α_{xx}	α_{yy}	α_{zz}	$\bar{\alpha}$
2	0.1017	0.7460	0.2826	0.1366	0.4973	0.9623	0.5321
3	0.1033	0.7815	0.2949	0.1410	0.5277	1.0356	0.5681
4	0.1047	0.7897	0.2981	0.1419	0.5369	1.0493	0.5760
5	0.1047	0.7914	0.2987	0.1419	0.5377	1.0547	0.5781
6	0.1047	0.7917	0.2988	0.1419	0.5378	1.0553	0.5783
7	0.1047	0.7918	0.2988	0.1419	0.5378	1.0554	0.5784
8	0.1047	0.7918	0.2988	0.1419	0.5378	1.0554	0.5784

for the polarizabilities (with differences with respect to eight HO basis functions results smaller than 0.0002 a.u.). If not stated differently we will in the following analyses exclusively use six HO basis functions and include all VSCF modals in the VCI calculations.

2. Convergence with respect to VCI excitation level

In Table II we report the pure vibrational contribution to the static polarizability of water and formaldehyde obtained using VSCF and VCI with maximum excitation from 1 to 6 (3 for water) using the converged one-mode basis of the previous section. The potential and property surfaces have been obtained using CCSD/aug-cc-pVTZ. While for water it is necessary to reach FVCI (i.e., VCI[3]) in order to obtain very accurate results, for formaldehyde the difference between VCI[3] and FVCI (i.e., VCI[6]) is smaller than 0.0005 a.u. for all components. Thereby, we will in the following use the VCI[3] mode-mode correlation level.

3. Convergence with respect to details of the potential and property surface

In Table III we report the pure vibrational contribution to the static polarizability for water obtained using FVCI and six HO basis functions for different potential and property surfaces. For the details of the property and potential surfaces we use the notation introduced in Ref. 30. We first discuss the convergence of the results with respect to the property surface given by a three-mode fourth order Taylor

(V[3M4T]) expansion for the potential. Here we observe that the results obtained at the P[1M2T] level (or even at P[1M1T]) seem to be very close to the most accurate predictions (P[3M4T]). However, this is somewhat fortuitous since including higher order terms in the 1M potential surfaces affects the α_{zz} component and actually leads to less accurate results than obtained by the P[1M1T] potential. Thus, for water the PV polarizability is found to be essentially converged at the P[2M3T] level. Concerning the variation in the potential we observe that almost converged results may be obtained at the V[2M4T] level. Finite field MP2/Pol FVCI calculations performed by Torrent-Sucarrat *et al.*³¹ showed that the inclusion of fifth and sixth order terms in the Taylor expansion for the potential (V[3M6T]) causes a decrease of 2% to the total vibrational polarizability (PV+ZPVA). Thus, we expect that our error due to the exclusion of such fifth and sixth order terms has a similar effect. In summary we find that the potential/property combination V[2M4T]/P[2M3T] (or P[2M4T]) gives very accurate results. However, acceptable results may be obtained using lower order property surfaces such as P[2M2T] or even P[1M2T].

In addition to the results obtained using CCSD/aug-cc-pVTZ potential and property surfaces we have also included V[3M4T]/P[3M4T] results based on CCSD(T)/aug-cc-pVTZ potential and property surfaces. We here observe that the effects of triples excitations in the electronic structure calculations are to lower the PV polarizabilities. For the isotropic polarizability this lowering amounts to $\sim 1.3\%$.

The results of the variational calculations in Table III

TABLE II. The static PV polarizability for water (V3M4T/P3M4T) and formaldehyde (V4M4T/P4M4T) calculated using VSCF, truncated VCI, and FVCI. The number of one-mode basis functions is six for water and formaldehyde. The potential and property surfaces have been obtained using CCSD/aug-cc-pVTZ. The results are in a.u.

	Water			Formaldehyde			
	α_{yy}	α_{zz}	$\bar{\alpha}$	α_{xx}	α_{yy}	α_{zz}	$\bar{\alpha}$
VSCF	0.1007	0.7815	0.2940	0.1371	0.4803	1.0491	0.5555
VCI[1]	0.1007	0.7792	0.2933	0.1371	0.4791	1.0441	0.5534
VCI[2]	0.1046	0.7821	0.2956	0.1399	0.5307	1.0457	0.5721
VCI[3]	0.1047	0.7917	0.2988	0.1419	0.5378	1.0553	0.5783
VCI[4]	0.1421	0.5382	1.0554	0.5786
VCI[5]	0.1422	0.5382	1.0555	0.5786
VCI[6]	0.1422	0.5382	1.0555	0.5786

TABLE III. The static FVCI PV polarizability for water calculated using different mode combinations and truncations levels in the mechanical and electrical potentials. The number of one-mode basis functions is six. Also included are the α^{nr} and $\alpha^{\text{nr}} + \alpha^{c\text{-ZPVA}}$ results (see text for details). The results are in a.u.

Model	α_{yy}	α_{zz}	$\bar{\alpha}$
CCSD/aug-cc-pVTZ V3M4T/P1M1T	0.109	0.789	0.299
CCSD/aug-cc-pVTZ V3M4T/P1M2T	0.109	0.792	0.300
CCSD/aug-cc-pVTZ V3M4T/P2M2T	0.104	0.780	0.295
CCSD/aug-cc-pVTZ V3M4T/P1M3T	0.109	0.804	0.304
CCSD/aug-cc-pVTZ V3M4T/P2M3T	0.105	0.792	0.299
CCSD/aug-cc-pVTZ V3M4T/P3M3T	0.105	0.792	0.299
CCSD/aug-cc-pVTZ V3M4T/P1M4T	0.109	0.804	0.304
CCSD/aug-cc-pVTZ V3M4T/P2M4T	0.105	0.792	0.299
CCSD/aug-cc-pVTZ V3M4T/P3M4T	0.105	0.792	0.299
CCSD/aug-cc-pVTZ V1M4T/P3M4T	0.010	0.749	0.253
CCSD/aug-cc-pVTZ V2M4T/P3M4T	0.104	0.793	0.299
CCSD/aug-cc-pVTZ V2M4T/P2M4T	0.105	0.793	0.299
CCSD/aug-cc-pVTZ V2M4T/P2M3T	0.105	0.794	0.300
CCSD/aug-cc-pVTZ V2M4T/P2M2T	0.104	0.782	0.295
CCSD/aug-cc-pVTZ V2M4T/P1M2T	0.109	0.793	0.301
CCSD(T)/aug-cc-pVTZ V3M4T/P3M4T	0.097	0.787	0.295
CCSD(T)/aug-cc-pVTZ α^{nr}	0.096	0.721	0.272
MP2/Pol α^{nr} (Ref. 31)		0.698	
MP2/Pol $\alpha^{\text{nr}} + \alpha^{c\text{-ZPVA}(l)}$ (Ref. 44)	0.094	0.764	0.286

may be compared to simpler approaches based on the perturbation theory approach of Bishop and Kirtman^{15,16,25} or the alternative nuclear relaxation procedure.^{26–29} The simplest of these, the so-called double-harmonic (DH) approximation,²⁵ which for α is equivalent to the nuclear relaxation contribution to the polarizability (α^{nr}),²⁸ considers a harmonic potential and a linear (one-mode) property surface. Literature values for the PV polarizability of water obtained using these simpler approaches have also been included in Table III. Here we find for α^{nr} that the yy component compares well with the more elaborate results, whereas the zz component is underestimated leading to an overall underestimation of 7.8% for the isotropic polarizability. Of course, the α^{nr} approximation would have a far worse performance for more anharmonic systems.³¹ In addition to our results for α^{nr} we have for comparison also included the results of α^{nr} obtained by Torrent-Sucarrat *et al.*³¹ and the $\alpha^{\text{nr}} + \alpha^{c\text{-ZPVA}(l)}$ results compiled from Ref. 44 based on MP2/Pol electronic structure calculations. As seen from Table III, the MP2 α^{nr} results are in fairly good agreement with the CCSD(T) predictions favoring MP2 as a cost efficient method for the evaluation of PV polarizabilities. From the point of view of the nuclear relaxation approach, $\alpha^{c\text{-ZPVA}(l)}$ is the first anharmonic correction to α^{nr} . The results presented in Table III show that, in complete agreement with our FVCI linear response results, when this correction is added to α^{nr} the value of the zz component of the PV polarizability increases by about 9%. Torrent-Sucarrat *et al.*³¹ also found an excellent agreement between variational and perturbation theory water vibrational polarizabilities, although their results were computed using finite field nuclear relaxation techniques instead of the analytical linear response method. However, for more anhar-

TABLE IV. The static VCI[3] PV polarizability for formaldehyde calculated using different mode combinations and truncations levels in the mechanical and electrical potentials. Also included are the corresponding α^{nr} results (see text for details). The number of one-mode basis functions is six. The results are in a.u.

Model	α_{xx}	α_{yy}	α_{zz}	$\bar{\alpha}$
CCSD/aug-cc-pVTZ V4M4T/P1M1T	0.142	0.471	1.005	0.539
CCSD/aug-cc-pVTZ V4M4T/P1M2T	0.142	0.471	1.006	0.540
CCSD/aug-cc-pVTZ V4M4T/P2M2T	0.147	0.524	1.014	0.561
CCSD/aug-cc-pVTZ V4M4T/P1M3T	0.140	0.468	1.017	0.542
CCSD/aug-cc-pVTZ V4M4T/P2M3T	0.142	0.540	1.058	0.580
CCSD/aug-cc-pVTZ V4M4T/P3M3T	0.142	0.540	1.057	0.580
CCSD/aug-cc-pVTZ V4M4T/P1M4T	0.140	0.468	1.016	0.541
CCSD/aug-cc-pVTZ V4M4T/P2M4T	0.142	0.539	1.055	0.579
CCSD/aug-cc-pVTZ V4M4T/P3M4T	0.142	0.538	1.055	0.578
CCSD/aug-cc-pVTZ V4M4T/P4M4T	0.142	0.538	1.055	0.578
CCSD/aug-cc-pVTZ V1M4T/P4M4T	0.131	0.450	1.013	0.531
CCSD/aug-cc-pVTZ V2M4T/P4M4T	0.142	0.536	1.062	0.580
CCSD/aug-cc-pVTZ V3M4T/P4M4T	0.142	0.540	1.055	0.579
CCSD/aug-cc-pVTZ V2M4T/P2M4T	0.142	0.537	1.062	0.580
CCSD/aug-cc-pVTZ V2M4T/P2M3T	0.142	0.538	1.064	0.581
CCSD/aug-cc-pVTZ V2M4T/P2M2T	0.147	0.522	1.046	0.572
CCSD/aug-cc-pVTZ V2M4T/P1M2T	0.142	0.470	1.013	0.542
CCSD(T)/aug-cc-pVTZ V4M4T/P4M4T	0.131	0.582	1.049	0.587
CCSD(T)/aug-cc-pVTZ α^{nr}	0.126	0.467	0.954	0.516
HF/Pol α^{nr} (Ref. 54)	0.79
MP2/aug-cc-pVTZ α^{nr} (Ref. 55)	0.927	0.493
MP2/Z3PolX α^{nr} (Ref. 55)	0.794	0.471

monic systems perturbation theory based procedures diverge and only explicit variational wave function methods give reliable results for vibrational polarizabilities.

Table IV reports similar calculations as considered above but for formaldehyde. We first discuss the convergence of the results with respect to the property surface given by a four-mode fourth order Taylor (V[4M4T]) expansion for the potential. Here we observe that it is necessary to go beyond one-mode couplings for high accuracy. Also, the order of the Taylor expansion is important. At the P[2M3T] level, the results are almost converged with respect to the P[4M4T] property surface (all components within 0.003 a.u.). Concerning the variation in the potential we observe that almost converged results are obtained at the V[2M4T] level (all components within 0.007 a.u.). These observations are similar to the case of water. In addition, the combination V[2M4T]/P[2M3T] (or P[2M4T]) is seen to provide very accurate results. Acceptable results are also obtained using V[2M4T]/P[2M2T] which is very attractive since the number of property calculations in this approach is reduced. Although it is necessary to investigate a far larger set of molecules to generalize these results, the V[2M4T]/P[2M2T] level allows a feasible computation of PV polarizabilities of larger molecular systems.

Finally, introducing triples excitations in the electronic structure calculations affects the PV polarizabilities, e.g., the isotropic PV polarizability is lowered $\sim 1.6\%$ as compared to potentials/property surfaces calculated using CCSD. This lowering is of the same magnitude as found for water. Concerning the performance of the double-harmonic approxima-

TABLE V. The frequency-dependent VCI[3] PV polarizability for water and formaldehyde calculated at selected frequencies. The number of one-mode basis functions is six and the results are based on CCSD(T)/aug-cc-pVTZ level potential and property surfaces at the V3M4T/P3M4T level for water and the V4M4T/P4M4T level for formaldehyde. The results are in a.u.

	Frequency	α_{xx}		α_{yy}		α_{zz}		$\bar{\alpha}$	
		VSCF	VCI[3]	VSCF	VCI[3]	VSCF	VCI[3]	VSCF	VCI[3]
Water	0.0000	0.000	0.000	0.093	0.097	0.777	0.787	0.290	0.295
	0.0010	0.000	0.000	0.094	0.097	0.792	0.803	0.295	0.300
	0.0428	0.000	0.000	-0.019	-0.023	-0.024	-0.024	-0.014	-0.016
	0.0656	0.000	0.000	-0.007	-0.008	-0.010	-0.010	-0.006	-0.006
	0.0856	0.000	0.000	-0.004	-0.005	-0.006	-0.006	-0.003	-0.003
Formaldehyde	0.0000	0.126	0.131	0.519	0.582	1.043	1.049	0.563	0.587
	0.0010	0.131	0.136	0.528	0.591	1.058	1.064	0.572	0.597
	0.0428	-0.002	-0.002	-0.038	-0.043	-0.052	-0.052	-0.031	-0.032
	0.0656	-0.001	-0.001	-0.015	-0.018	-0.021	-0.021	-0.012	-0.013
	0.0856	-0.000	-0.000	-0.009	-0.010	-0.012	-0.012	-0.007	-0.007

tion we find that all components of α^{nr} are underestimated as compared to the linear response function results leading to an overall underestimation of the isotropic PV polarizability. Table IV includes in addition to our findings also some literature values for the static α^{nr} . As for water, we find that predictions relying on MP2 electronic structure calculations are in fairly good agreement with the results based on CCSD(T). However, as is well known,^{45,46} Hartree-Fock is not a reliable method to calculate PV polarizabilities. For formaldehyde using potentials and property surfaces derived on the basis of Hartree-Fock calculations leads to a PV isotropic polarizability which is $\sim 50\%$ higher in magnitude than our CCSD(T) α^{nr} predictions. Thus, inclusion of electronic correlation effects is found to be mandatory.

4. Frequency dependence of the pure vibrational contribution

In Table V we give the PV polarizabilities of water and formaldehyde for selected frequencies calculated using VSCF or VCI[3] and in both cases six HO one-mode basis functions. The potentials and property surfaces used are V[3M4T]/P[3M4T] for water and V[4M4T]/P[4M4T] for formaldehyde both at the CCSD(T)/aug-cc-pVTZ level. From Table V we observe, as expected, that the PV polarizability is significant in the static or low frequency (IR) region but tends to zero for optical frequencies.⁴⁷⁻⁴⁹ Thus, already around a frequency equal to 0.0428 a.u. (1064 nm) the PV contribution is very small and essentially negligible. Also we observe that the PV polarizability changes sign, e.g., for higher frequencies this becomes negative. Obviously, the dispersion of the PV contribution is very different from the dispersion of the ZPVA which may, to a high precision, be represented by a polynomial expansion in the frequency.

Comparison of our theoretical results with experimental data is hampered by the fact that the static polarizabilities are usually derived by an extrapolation to zero frequency of experimental refractivity data. However, since the PV contribution tends to be zero in the range of optical frequencies, the “experimental” static component will in this case not contain any contribution from the PV polarizability. For formalde-

hyde, however, an experimental value for the isotropic polarizability has been derived on the basis of absolute dipole photoabsorption spectra⁵⁰ and found to be 18.69 a.u. In Ref. 30 we calculated the static ZPVA isotropic polarizability to be 18.035 a.u. on the basis of FVCI using V[4M4T]/P[4M4T] CCSD/aug-cc-pVTZ potential/polarizability surfaces. Adding to this number the PV contribution from this work we find the total static polarizability to be 18.622 a.u. in perfect agreement with the experimental result. It should, however, be noticed that the ZPVA isotropic polarizability does not include the effects of triples excitations which, for water, has been found to slightly lower the electronic equilibrium component.⁵¹

B. Sum-over-states results

1. Convergence with respect to the number of vibrational states

The VCI response functions are easily separated into contributions from different states by construction of response functions explicitly from excited state wave functions i.e., by evaluating the response functions in the spectral (SOS) representation [Eq. (5)]. We shall now show how the frequency-dependent vibrational polarizability converges for water and formaldehyde. When convergence can be easily obtained the SOS expression provides a convenient approach to obtain vibrational frequency dispersion curves. In particular, we shall show how the effect of introducing a finite vibrational excited state lifetime via a damping factor into the linear response function can be investigated using this approach.

In Fig. 1 we have shown the convergence of the nonzero components of the polarizability tensor from below, with respect to the number of vibrational states included in order of increasing energy. Convergence is relatively fast and the frequency-dependent polarizability is fully converged with about 20 states. Of course, the SOS converged result completely agrees with the LR results presented in previous sections. The convergence pattern is identical regardless of the applied frequency; we see that for both $\omega=0$ and $\omega \neq 0$ that α_{yy} and α_{zz} converge in the same manner. The level parts of

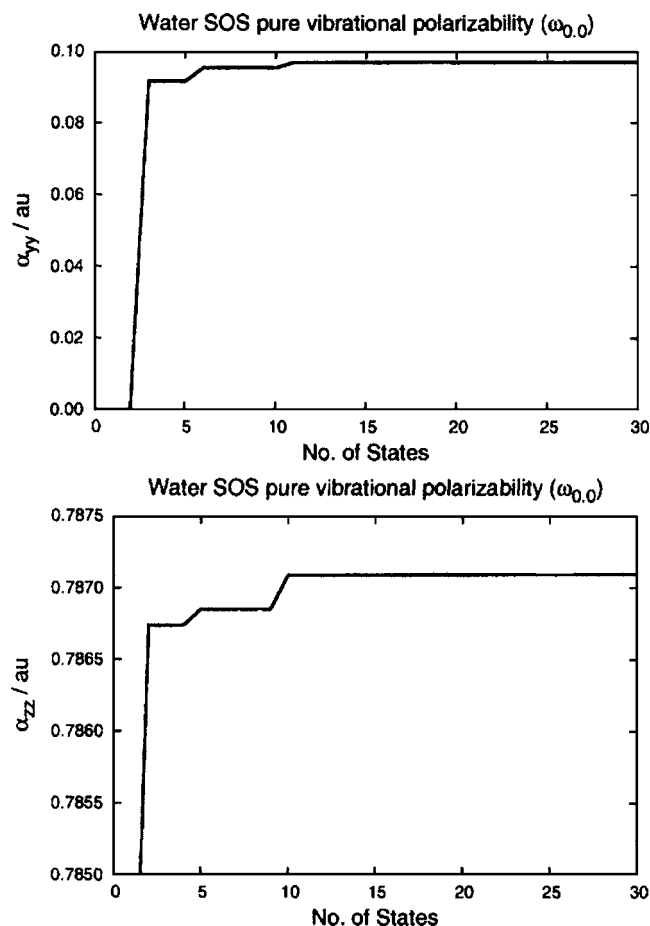


FIG. 1. Convergence of the sum-over-states contributions to the nonzero components of the static pure vibrational polarizability tensor for water.

the curve arise due to the fact that states are added in order of increasing energy and some states make a zero contribution (i.e., have zero transition moments) by symmetry.

In Fig. 2 we have shown the convergence for the three nonzero components of the vibrational polarizability tensor for formaldehyde. It can be seen that the convergence is slightly slower for formaldehyde than for water. This is due to the increase in vibrational degrees of freedom giving rise to a greater number of excited states at not too high energy contributing to the property. Similar to water the convergence at nonresonant frequencies is almost identical to the static case.

2. Frequency dispersion

The poles in the pure vibrational frequency-dependent polarizability occur at vibrational excitation energies. Figure 3 shows the frequency dispersion for the pure vibrational isotropic polarizability ($\bar{\alpha}$) of water. The poles indicated occur at the fundamental vibrational frequencies, and the first two overtones. Higher excitations, corresponding to further overtones and combinations, are extremely sharp and are not shown. The poles of Eq. (5) formally give the excitation energies but do not take account of the fact that excited states have a finite lifetime. Such a concept can be introduced phenomenologically via a damping factor (γ for simplicity taken to be the same for all states),^{52,53}

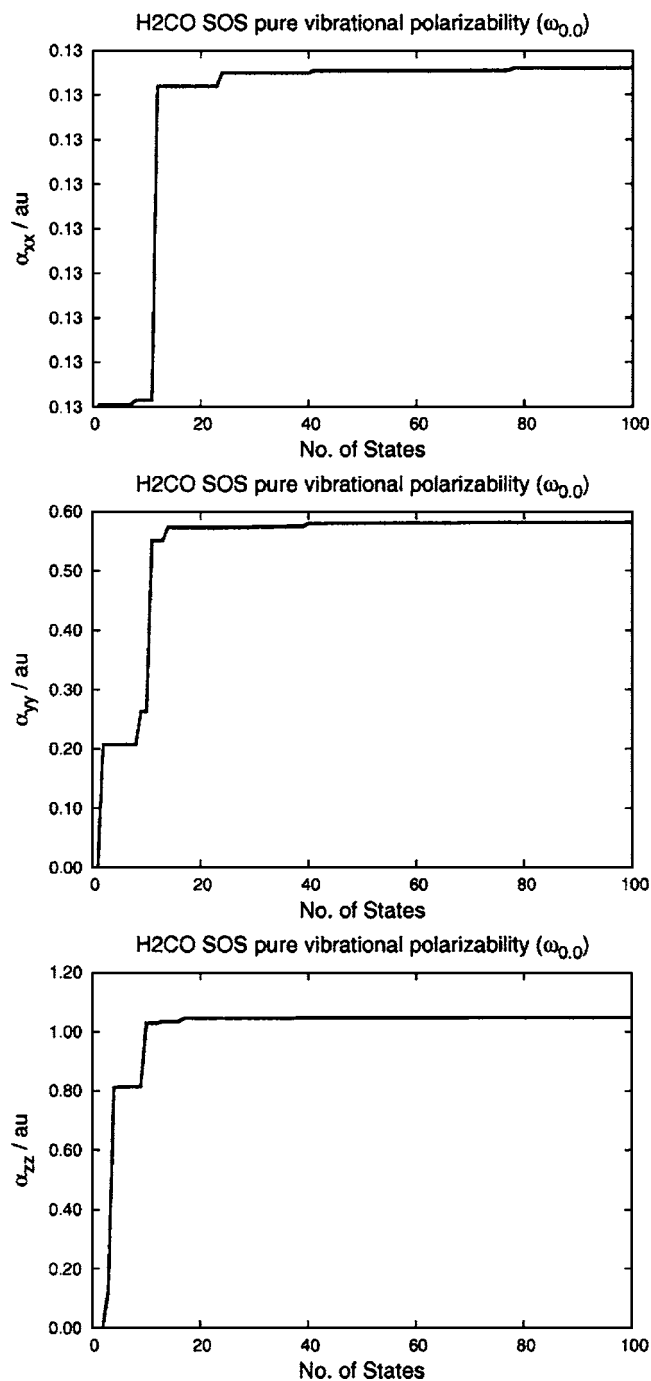


FIG. 2. Convergence of the sum-over-states contributions to the nonzero components of the static pure vibrational polarizability tensor for formaldehyde.

$$\langle\langle X, Y \rangle\rangle_{\omega_y} = \sum_k \frac{\langle\Psi_o|X|\Psi_k\rangle\langle\Psi_k|Y|\Psi_o\rangle(\omega_y - \omega_k)}{(\omega_y - \omega_k)^2 + \gamma^2} - \frac{\langle\Psi_o|X|\Psi_k\rangle\langle\Psi_k|Y|\Psi_o\rangle(\omega_y + \omega_k)}{(\omega_y + \omega_k)^2 + \gamma^2}. \quad (29)$$

Clearly when $\gamma=0$, Eq. (29) reduces to Eq. (5), but when $\gamma \neq 0$, the response function becomes finite even when $\omega_y = \pm \omega_k$. Two values of γ are shown in Figs. 3(b) and 3(c) across the first pole (corresponding to the bending fundamental). For $\gamma=0.5 \text{ cm}^{-1}$ the pole is still quite sharp and localized, whereas for $\gamma=22 \text{ cm}^{-1}$ the pole becomes more

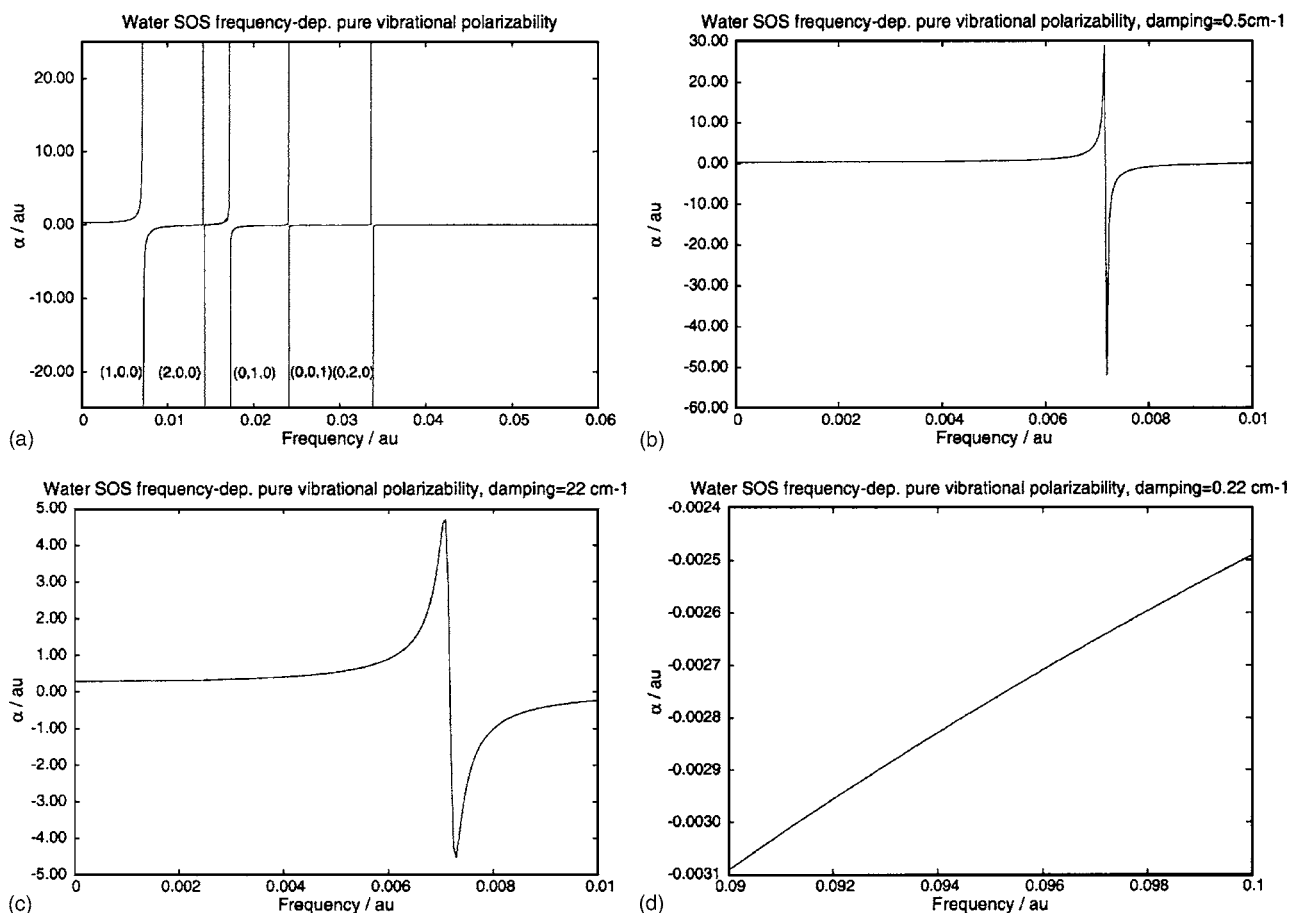


FIG. 3. Water: (a) The isotropic pure vibrational polarizability as a function of frequency. The poles shown are for the fundamentals and first two overtones. (b) The isotropic pure vibrational polarizability frequency dispersion across the first pole including a small (0.5 cm^{-1}) damping factor, causing the pole to become finite, (c) an increased damping factor causing the pole to become more delocalized and have a much smaller magnitude, and (d) the high-frequency end of the curve, which even at very high resolution shows no observable pole structure, even though it crosses many very highly excited vibrational states.

spread. Figure 3(d) shows the frequency dispersion at very high frequencies across several poles representing extremely highly excited vibrational states (approximately states 89–100 in FVCI). It is clear that at such high frequencies the poles are essentially infinitely narrow and are not observable on the dispersion curve. Thus, the higher frequency vibrational dispersion curve is flat when only a very small damping factor is included.

Finally, in Figs. 4 and 5 we have shown the total polarizability frequency dispersion. The total polarizability is defined as the sum of the vibrationally averaged ground-state electronic polarizability plus the pure vibrational contribution. Techniques for obtaining the vibrationally averaged ground-state electronic polarizability have been developed in Ref. 30, and computed for water and formaldehyde. Here, we compute the total polarizability as the sum of the isotropic vibrational polarizability and the isotropic vibrationally averaged electronic polarizability obtained from the dispersion curve from Ref. 30. For the smallest value ($\gamma=0.22 \text{ cm}^{-1}$) we still see overtone poles. Increasing ($\gamma=22 \text{ cm}^{-1}$ and $\gamma=220 \text{ cm}^{-1}$) for water clearly causes the dispersion curve to “smooth out” and the poles due to overtone and higher excitations disappear. The same is observed for formaldehyde (Fig. 5), although with a small damping there are many more poles in the low-frequency region.

The frequency dependence found in Figs. 4 and 5 is an almost textbooklike illustration of the frequency dependence of the combined electronic and vibrational polarizability showing that the pure vibrational contribution is significant for the static case, has some dominating poles at vibrational frequencies, but gives very small (usually negligible) contributions for optical frequencies.

VI. SUMMARY AND OUTLOOK

We have reported the implementation of linear response theory for a vibrational configuration interaction (VCI) wave function. It was described how the VCI response function approach can be efficiently implemented using VCI direct techniques. We have presented sample calculations for water and formaldehyde investigating various aspects of the calculation of pure vibrational polarizabilities. In particular, we have studied the convergence of the PV polarizabilities with respect to one-mode HO basis set, VCI excitation level, and potential and property surfaces. Furthermore, the frequency dependence of the vibrational wave function and the convergence of sum-over-states calculations have also been investigated. VCI[3] using six HO basis functions and V[2M4T]/P[2M4T] surfaces was found to give very accurate PV polarizability results for water and formaldehyde.

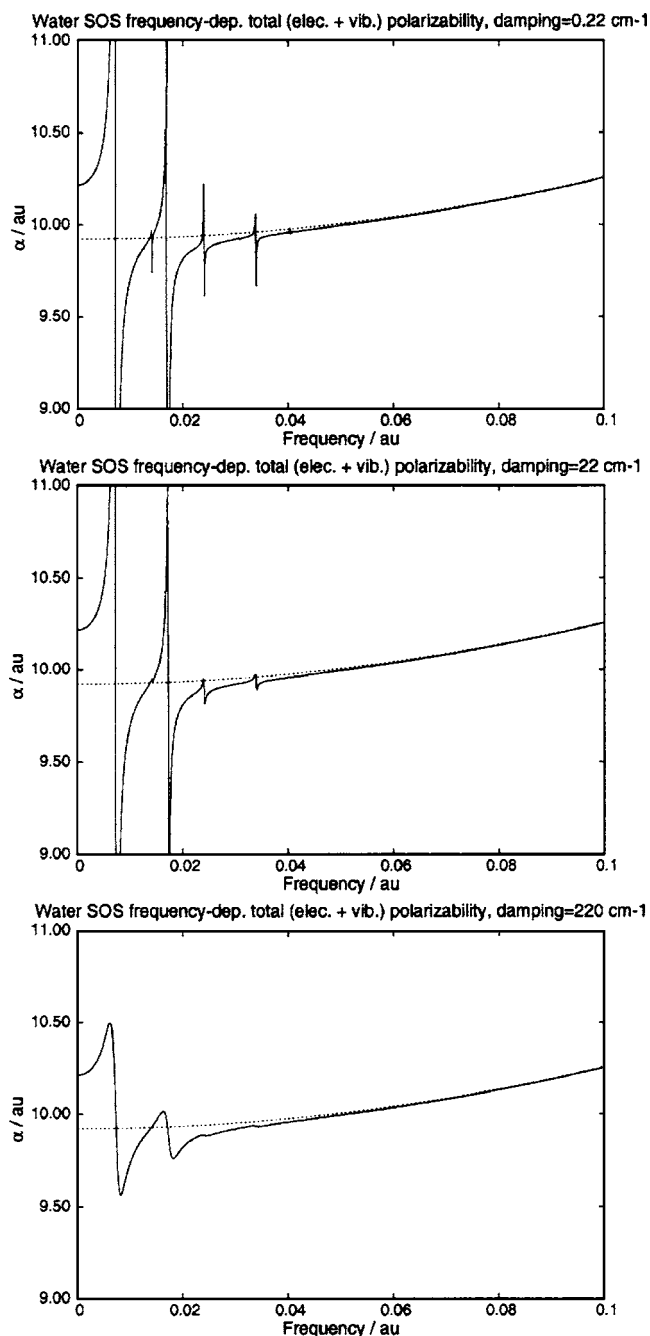


FIG. 4. The total polarizability of water as a function of frequency with three damping factors. This is defined as the sum of the zero-point vibrationally averaged electronic polarizability obtained from the dispersion curve optimized in Ref. 30 [$\bar{\alpha}(\omega)=9.923(1+3.3766\omega^2)$ —dashed line] plus the pure vibrational component. The vibrational component is clearly only important at low frequencies, and gives rise to a significant static component.

For water and formaldehyde we have presented detailed studies of the frequency dependence of the vibrational response functions illustrating the potentially rather complicated pole structure of the vibrational linear response function, but also that for optical frequencies the pure vibrational contribution to the polarizability becomes essentially zero. For small systems that are not highly anharmonic such as water and formaldehyde, the convergence of the sum-over-states expansion is reasonable. The sum-over-states approach thereby provides a possible way to investigate the frequency

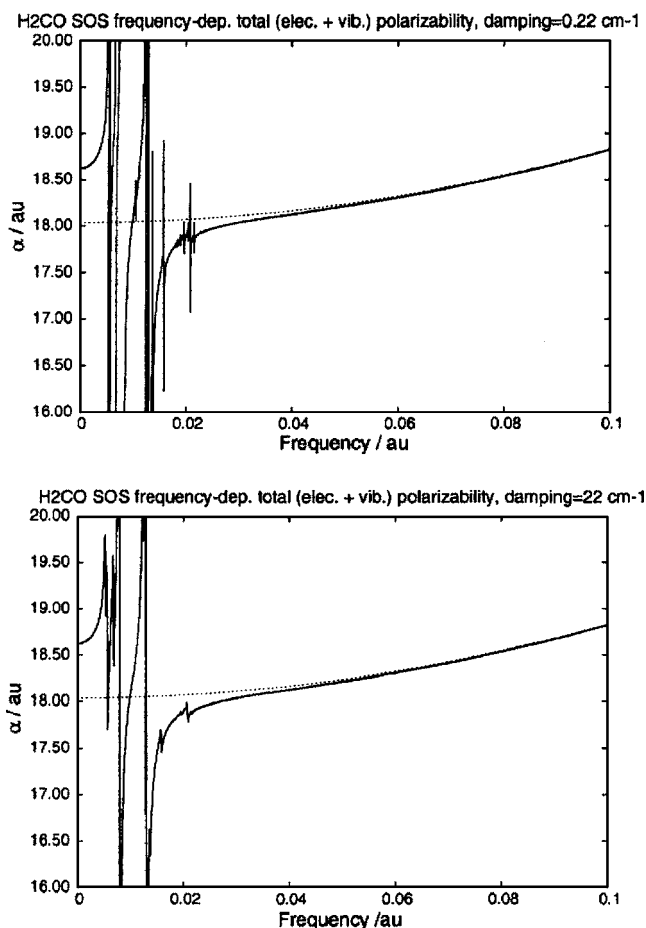


FIG. 5. The total polarizability of formaldehyde as a function of frequency with two damping factors. This is defined as the sum of the zero-point vibrationally averaged electronic polarizability obtained from the dispersion curve optimized in Ref. 30 [$\bar{\alpha}(\omega)=18.035(1+4.4146\omega^2)$ —dashed line] plus the pure vibrational component. The vibrational component is clearly only important at low frequencies, and gives rise to a significant static component.

dependence of the linear response function, and using this approach we have illustrated that accounting phenomenologically for the limited lifetime of the excited states a smoothing of the frequency dependence is obtained. Though the sum-over-states approach was not prohibitive for water and formaldehyde it is in general a rather slowly converging procedure with respect to the number of states included, making it inefficient compared to the analytical response approach. For example, for the total static polarizability tensor, the necessary linear response functions can be obtained by solving only three sets of linear equations in addition to optimizing the ground state. In contrast the sum-over-states approach will require the construction of many excited states for getting close to the same accuracy.

In subsequent works we shall generalize the theory and implementation to the calculation of higher order vibrational response properties and other types of vibrational wave functions. We also plan to combine the analytical response formulas with the finite field approach to calculate dynamic pure vibrational second hyperpolarizabilities. The results also indicates that the inclusion of a phenomenological damping due to the finite lifetime of the excited vibrational

states might be relevant for studying frequency-dependent vibrational properties. Such methods have already been developed for some electronic structure response methods,¹² and it is probably possible to develop similar methods for vibrational structure response methods.

ACKNOWLEDGMENTS

This work has been supported by the Danish Research Agency, the Danish National Research Foundation, and DCSC (Danish Center for Super Computing). One of the authors (J.M.L.) acknowledges financial support from the Generalitat de Catalunya through the BE2004 program.

- ¹J. M. Bowman, S. Carter, and X. C. Huang, *Int. Rev. Phys. Chem.* **22**, 533 (2003).
- ²G. Rauhut, *J. Chem. Phys.* **121**, 9313 (2004).
- ³B. Brauer, R. B. Gerber, M. Kabelac, P. Hobza, J. M. Bakker, A. G. A. Riziq, and M. S. de Vries, *J. Phys. Chem. A* **109**, 6974 (2005).
- ⁴K. Yagi, K. Hirao, T. Taketsugu, and M. S. Gordon, *J. Chem. Phys.* **121**, 1283 (2004).
- ⁵*Computational Molecular Spectroscopy*, edited by P. Jensen and P. R. Bunker (Wiley, Chichester, 2000).
- ⁶O. Christiansen, *J. Chem. Phys.* **120**, 2140 (2004).
- ⁷O. Christiansen, *J. Chem. Phys.* **120**, 2149 (2004).
- ⁸O. Christiansen, *J. Chem. Phys.* **122**, 194105 (2005).
- ⁹J. Olsen and P. Jørgensen, *J. Chem. Phys.* **82**, 3235 (1985).
- ¹⁰J. Olsen and P. Jørgensen, in *Modern Electronic Structure Theory*, edited by D. R. Yarkony, (World Scientific, Singapore, 1995), Vol. 2, Chap. 13, pp. 857–990.
- ¹¹O. Christiansen, P. Jørgensen, and C. Hättig, *Int. J. Quantum Chem.* **68**, 1 (1998).
- ¹²P. Norman, D. M. Bishop, H. J. A. Jensen, and J. Oddershede, *J. Chem. Phys.* **115**, 10323 (2001).
- ¹³L. Barron, *Molecular Light Scattering and Optical Activity*, 2nd ed. (Cambridge University Press, Cambridge, 2004).
- ¹⁴D. Long, *The Raman Effect. A Unified Treatment of the Theory of Raman Scattering by Molecules* (Wiley, Chichester, 2002).
- ¹⁵R. Bishop, *Theor. Chim. Acta* **80**, 95 (1991).
- ¹⁶D. M. Bishop and B. Kirtman, *J. Chem. Phys.* **97**, 5255 (1992).
- ¹⁷B. Champagne, M. Spassova, J. B. Jadin, and B. Kirtman, *J. Chem. Phys.* **116**, 3935 (2002).
- ¹⁸O. Quinet, B. Kirtman, and B. Champagne, *J. Chem. Phys.* **118**, 505 (2003).
- ¹⁹M. Torrent-Sucarrat, M. Sola, M. Duran, J. M. Luis, and B. Kirtman, *J. Chem. Phys.* **120**, 6346 (2004).
- ²⁰A. Avramopoulos, H. Reis, J. B. Li, and M. G. Papadopoulos, *J. Am. Chem. Soc.* **126**, 6179 (2004).
- ²¹O. P. Andrade, A. Aragao, O. A. V. Amaral, T. L. Fonseca, and M. A. Castro, *Chem. Phys. Lett.* **392**, 270 (2004).
- ²²M. R. Pederson, T. Baruah, P. B. Allen, and C. Schmidt, *J. Chem. Theory Comput.* **1**, 590 (2005).
- ²³E. Squitieri and I. Benjamin, *Chem. Phys.* **326**, 363 (2006).
- ²⁴R. Zalesny and W. Bartkowiak, *Int. J. Quantum Chem.* **104**, 660 (2005).
- ²⁵D. M. Bishop, *Adv. Chem. Phys.* **104**, 1 (1998).
- ²⁶D. M. Bishop, M. Hasan, and B. Kirtman, *J. Chem. Phys.* **103**, 4157 (1995).
- ²⁷J. M. Luis, J. Marti, M. Duran, J. L. Andres, and B. Kirtman, *J. Chem. Phys.* **108**, 4123 (1998).
- ²⁸J. M. Luis, M. Duran, and J. L. Andres, *J. Chem. Phys.* **107**, 1501 (1997).
- ²⁹B. Kirtman, J. M. Luis, and D. M. Bishop, *J. Chem. Phys.* **108**, 10008 (1998).
- ³⁰J. Kongsted and O. Christiansen, *J. Chem. Phys.* **125**, 124108 (2006).
- ³¹M. Torrent-Sucarrat, J. M. Luis, and B. Kirtman, *J. Chem. Phys.* **122**, 204108 (2005).
- ³²J. M. Bowman, K. M. Christoffel, and F. Tobin, *J. Phys. Chem.* **83**, 905 (1979).
- ³³K. M. Christoffel and J. M. Bowman, *Chem. Phys. Lett.* **85**, 220 (1982).
- ³⁴J. M. Bowman, *Acc. Chem. Res.* **19**, 202 (1986).
- ³⁵S. Carter, J. M. Bowman, and N. C. Handy, *Theor. Chim. Acta* **100**, 191 (1998).
- ³⁶R. B. Gerber and M. A. Ratner, *Adv. Chem. Phys.* **70**, 97 (1988).
- ³⁷O. Christiansen, C. Hättig, and J. Gauss, *J. Chem. Phys.* **109**, 4745 (1998).
- ³⁸K. Sasagane, F. Aiga, and R. Itoh, *J. Chem. Phys.* **99**, 3738 (1993).
- ³⁹B. O. Roos, *Chem. Phys. Lett.* **15**, 153 (1972).
- ⁴⁰T. Helgaker, P. Jørgensen, and J. Olsen, *Molecular Electronic Structure Theory* (Wiley, Chichester, 2000).
- ⁴¹E. R. Davidson, *J. Comput. Phys.* **17**, 87 (1975).
- ⁴²O. Christiansen, *J. Chem. Phys.* **119**, 5773 (2003).
- ⁴³O. Christiansen, MIDASCP (molecular interactions, dynamics and simulation chemistry program package in C++), University of Aarhus, 2006, with contributions from J. Kongsted and M. J. Paterson.
- ⁴⁴H. Reis, S. Raptis and M. Papadopoulos, *Chem. Phys.* **263**, 301 (2001).
- ⁴⁵H. Reis, M. G. Papadopoulos, and A. Avramopoulos, *J. Phys. Chem. A* **107**, 3907 (2003).
- ⁴⁶M. Torrent-Sucarrat, M. Sola, M. Duran, J. M. Luis, and B. Kirtman, *J. Chem. Phys.* **118**, 711 (2003).
- ⁴⁷D. Bishop and E. Dalskov, *J. Chem. Phys.* **104**, 1004 (1996).
- ⁴⁸O. Quinet and B. Champagne, *J. Chem. Phys.* **109**, 10594 (1998).
- ⁴⁹J. Luis, M. Duran, and B. Kirtman, *J. Chem. Phys.* **115**, 4473 (2001).
- ⁵⁰G. Cooper, J. E. Anderson, and C. E. Brion, *Chem. Phys.* **209**, 61 (1996).
- ⁵¹O. Christiansen, J. Gauss, and J. F. Stanton, *Chem. Phys. Lett.* **305**, 147 (1999).
- ⁵²P. N. Butcher and D. Cotter, *The Elements of Nonlinear Optics* (Cambridge University Press, Cambridge, 1993).
- ⁵³A. D. Buckingham and P. Fischer, *Phys. Rev. A* **61**, 035801 (2000).
- ⁵⁴A. Alparone and S. Millefiori, *Chem. Phys. Lett.* **416**, 282 (2005).
- ⁵⁵R. Zalesny and W. Bartkowiak, *Int. J. Quantum Chem.* **104**, 660 (2005).